

**3-D IMAGING OF INHOMOGENEOUS MATERIALS LOADED INSIDE
RECTANGULAR WAVEGUIDE BY NEWTON'S METHOD**

**M.Sc. Thesis by
Emre KILIÇ**

Department : Electronics and Telecommunications Engineering

Programme : Telecommunications Engineering

JUNE 2010

**3-D IMAGING OF INHOMOGENEOUS MATERIALS LOADED INSIDE
RECTANGULAR WAVEGUIDE BY NEWTON'S METHOD**

**M.Sc. Thesis by
Emre KILIÇ
(504081312)**

**Date of submission : 07 May 2010
Date of defence examination : 08 June 2010**

**Supervisor (Chairman) : Assoc. Prof. Dr. Ali YAPAR (ITU)
Members of the Examining Committee : Assis. Prof. Dr. Özgür ÖZDEMİR
(ITU)
Assis. Prof. Dr. Tanju YELKENÇİ
(MU)**

JUNE 2010

İSTANBUL TEKNİK ÜNİVERSİTESİ ★ FEN BİLİMLERİ ENSTİTÜSÜ

**DİKDÖRTGEN DALGA KILAVUZU İÇERİSİNDE
İNHOMOJEN CİSİMLERİN 3 BOYUTLU GÖRÜNTÜLENMESİ**

**YÜKSEK LİSANS TEZİ
Emre KILIÇ
(504081312)**

Tezin Enstitüye Verildiği Tarih : 07 Mayıs 2010

Tezin Savunulduğu Tarih : 08 Haziran 2010

**Tez Danışmanı : Doç. Dr. Ali Yapar (İTÜ)
Diğer Jüri Üyeleri : Yrd. Doç. Dr. Özgür ÖZDEMİR (İTÜ)
Yrd. Doç. Dr. Tanju YELKENCİ (MÜ)**

HAZİRAN 2010

FOREWORD

I would like to thank Associate Professor Doctor Ali Yapar, who gave me the opportunity to work under his supervision, for his precious guidance and motivation in accomplishing this thesis study.

I also would like to express my gratitude to Associate Professor Doctor Funda Akleman who never hesitated to help me when I needed his assistance and scientific contribution to my studies.

I am deeply indebted to both Professor Yapar and Professor Akleman for their never ending enthusiasm towards scientific research and for being role models that will always guide me through my academic career.

I would also like to thank my family for their invaluable moral auspices and their endless faith in me.

Finally; I would like to thank TUBITAK (The Scientific and Technological Research Council of Turkey) for supporting me financially by the project 108E146.

June 2010

Emre KILIÇ

Telecommunication Engineering

TABLE OF CONTENTS

	<u>Page</u>
LIST OF FIGURES	ix
SUMMARY	xi
ÖZET.....	xiii
1. INTRODUCTION.....	1
2. STATEMENT OF THE PROBLEM	5
2.1 Integral Representations	5
2.2 Dyadic Green's Function of Empty Rectangular Waveguide	7
2.3 Discretisation.....	8
3. INVERSE SCATTERING	11
3.1 Initial Guess.....	11
3.2 Newton Based Reconstruction Algorithm.....	13
3.3 Numerical and Experimental Results	15
4. CONCLUSION.....	25
REFERENCES.....	27
CURRICULUM VITA	29

LIST OF FIGURES

	<u>Page</u>
Figure 2.1 : Geometry of the problem: An inhomogeneous material which is placed in a rectangular waveguide (a)longitudinal view (b)cross-section view	5
Figure 3.1 : Exact and reconstructed profiles of an inhomogeneous material having linearly varying real part for five different y slices.	17
Figure 3.2 : Exact and reconstructed profiles of an inhomogeneous material having linearly varying imaginary part for five different y slices.	17
Figure 3.3 : Exact and reconstructed profiles of three layer material : real part for five different y slices.....	18
Figure 3.4 : Exact and reconstructed profiles of three layer material : imaginary part for five different y slices.....	18
Figure 3.5 : Exact and reconstructed profiles of an inhomogeneous material having 2-D sharp variations for $\xi=0.03$ and $f=6GHz$	20
Figure 3.6 : Exact and reconstructed profiles of an inhomogeneous material having 2-D sharp variations for $\xi=0.1$ and $J=6$ in a range of $f=6-7GHz$	20
Figure 3.7 : Exact and reconstructed profiles of an inhomogeneous material having 2-D sharp variations for $\xi=0.03$ and $f=9GHz$	21
Figure 3.8 : Real part of reconstructed versus mesh points when backpropagation algorithm is used.....	22
Figure 3.9 : Imaginary part of reconstructed versus mesh points when backpropagation algorithm is used.....	22
Figure 3.10 : Real part of reconstructed versus mesh points when initial guess is chosen manually	23
Figure 3.11 : Imaginary part of reconstructed versus mesh points when initial guess is chosen manually.	23

3-D IMAGING OF INHOMOGENEOUS MATERIALS LOADED INSIDE RECTANGULAR WAVEGUIDE BY NEWTON'S METHOD

SUMMARY

In this study, an iterative method based on Newton algorithm for the reconstruction of complex object function of the isotropic, inhomogeneous and arbitrary shaped materials loaded in a rectangular waveguide is addressed. By using the Dyadic Green's function of an empty rectangular waveguide, the problem is formulated as a system of integral equations consist of the well known data and object equations. While the data equation defines the nonlinear relation between unknown object function of the dielectric material and scattered field that is assumed to be measured, the object equation connects the unknown object function and the unknown total electric field inside the material. Two unknowns of this system, namely, the object function and the total electric field are solved in an iterative fashion by linearizing the nonlinear data equation in the sense of Newton method which corresponds to a first order Taylor expansion of the data equation with respect to the unknown object function. Since the problem is severely ill-posed like the other inverse problems, in order to obtain stable results, the data equation is regularized in the sense of Tikhonov for which regularization parameter is determined by Morozov discrepancy rule. For numerical applications, the continuous equations are discretized to reduce the problem into matrix systems via Method of Moments. The capabilities and validation limits of the method has been demonstrated with numerical simulations. Also, the proposed method is tested against experimental data and satisfactory reconstruction is obtained.

DİKDÖRTGEN DALGA KILAVUZU İÇERİSİNDE İNHOMOJEN CİSİMLERİN 3 BOYUTLU GÖRÜNTÜLENMESİ

ÖZET

Bu çalışmada dikdörtgen dalgakılavuzu içerisine yerleştirilmiş izotropik, inhomojen, keyfi bir geometriye sahip malzemelerin kompleks cisim fonksiyonun bulunması için Newton metoduna dayanan iteratif bir yöntem sunulmuştur. Boş dikdörtgen dalgakılavuzunun Dyadik Green fonksiyonu yardımıyla, problem, veri ve cisim denklemlerinden oluşan bir integral denklem sistemi ile formüle edilmiştir. Veri denklemi dielektrik malzemenin cisim fonksiyonu ile ölçüldüğü kabul edilen saçılan alan arasındaki doğrusal olmayan ilişkiyi tanımlar iken, cisim denklemi, bilinmeyen cisim fonksiyonu ile toplam elektrik alanı birbirine doğrusal bir şekilde bağlamaktadır. Bu integral sistemin iki bilinmeyeni, yani, cisim fonksiyonu ve toplam elektrik alan, veri denkleminin Newton yöntemiyle doğrusallaştırması, ki söz konusu denklemin cisim fonksiyonuna göre birinci mertebeden Taylor açılımına karşı düşmektedir, ile iteratif bir şekilde bulunmuştur. Diğer ters problemler gibi, söz konusu problemde oldukça kötü konumlanmış olduğundan, kararlı sonuçlar elde edebilmek için, veri denklemi Tikhonov anlamında düzenlenmiştir. Tikhonov için gerekli olan düzenleme parametresi Morozov aykırılık prensibi ile hesaplanmıştır. Sayısal uygulamalar için, sürekli denklemler Momentler yöntemiyle ayrıklaştırılarak matris denkleme indirgenmiştir. Çeşitli sayısal simülasyonlar ile, yöntemin yeterliliği ve çalışma bölgesi belirlenmiştir. Ayrıca söz konusu yöntem deneysel veriye karşıda denenmiş ve tatminkar sonuçlar elde edilmiştir.

1. INTRODUCTION

Determination of complex constitutive parameters of lossy dielectric materials is a very important topic in electromagnetic and microwave theory due to its wide range of applications in the areas of microwave devices, material test and measurements, fabrication of multilayered structures, non-destructive testing and biomedical applications, etc. It is possible to classify the solution techniques for the determination of electromagnetic parameters into two basic categories depending on the domain in which the material under test is located: free space and waveguide methods. In the open literature, one can find numerous studies that mainly aim to find electromagnetic parameters of (in)homogeneous material which can be classified as free space methods. These techniques are mainly based on classical approaches in inverse scattering formulation such as Born approximations, Newton method, contrast source inversion and linear sampling [1-6], or bio-inspired techniques such as neural network algorithm and genetic algorithms [7,8], etc.

On the other hand the waveguide gives a different set of challenges than corresponding problem in free space due to its particular geometry [9]. The most important advantage of waveguide techniques is that very few data sets could be enough for satisfactory reconstruction. Furthermore, waveguide experiments are considerably easier and cheaper than experiments of free space. On the contrary, there are also some disadvantages of waveguide techniques. A practical disadvantage is that any dimension of the dielectric material must not be greater than the dimensions of waveguide. Secondly, since particular geometry of the waveguide allows only a finite number of modes propagate and the other modes decay rapidly as a function of distance, the illposedness of inverse scattering problem of guided waves considerably increases [10].

For waveguide methods, although it is possible to find many bioinspired based techniques for the determination of electromagnetic parameters; to the best of our knowledge, classical inverse scattering techniques such as integral equation formulations applied to waveguide problem are very few under strict assumptions.

For example, the methods in [11-13] that based on the expression of propagation constant inside the material in terms of scattering parameters of the structure under test are restricted to homogeneous or multilayered case. In [14], an integral equation technique which is more complex than previous studies allows complex permittivity of the material at most be function of longitudinal axes and the dielectric material must be full loaded in the crosssection of waveguide.

A similar situation is valid for bio-inspired algorithms applied to waveguide problem. For instance, in [15] genetic algorithm which is combined with gradient descent optimization method is applied to homogeneous or layered materials having different shapes and positions. A neural network approach is successfully applied for two dimensional variations by using a priori information in [16].

The more general and inclusive problem in this respect is the reconstruction of the complex permittivity distribution of an arbitrary shaped inhomogeneous material loaded in a waveguide. To the best of our knowledge this problem have not been enough investigated in the open literature and it is open to new theoretical as well as experimental contributions. Within this framework, the goal of this study is to address the theoretical and numerical analysis of 3-D imaging problem related to inhomogeneous lossy materials located in a rectangular waveguide by an inverse scattering formalism. To this aim an empty rectangular waveguide is filled with an inhomogeneous material. The problem is then formulated as an inverse scattering one by considering the well known data and object equations which are written in terms of the object function and the electric field distribution in the waveguide. In the application of the method, firstly, initial values which is required for linearization of nonlinear data equation with respect to unknown object function is obtained by the aid of backpropagation algorithm [17]. Using two term Taylor expansion of nonlinear data equation with respect to the object function yields Newton iteration. Since there are two unknowns in formulation, the object equation is used in each iteration to obtain separately two unknowns, namely, the object function and the electric field distribution. This iteration scheme is continued until a desired level of accuracy is obtained. Since the data equation is an ill-posed one Tikhonov regularization in each iteration step is applied where the regularization parameter is calculated by Morozov's discrepancy principle.

In order to show the applicability as well as the limitations of the method some illustrative numerical examples are presented. The preliminary numerical examples showed that this conventional basic method which is comprehensively applied to open region problems is also applicable to a waveguide problem even in the case of very limited number of data. Although the method yields quite satisfactory results especially for smooth and continuous variations, it is very sensitive to the sharp changes in both geometrical and physical properties of the material and thus it is though promising but not fully capable of imaging such structures. From numerical results, it can be shown that multi-frequency measurements make the method robust against noisy data and use of higher modes, namely, higher frequency is a very efficient tool to improve the resolution of the method considerably. Finally, the proposed method for homogeneous case is tested against experimental data and satisfactory reconstruction is observed.

2. STATEMENT OF THE PROBLEM

2.1 Integral Representations

We consider a non-magnetic ($\mu = \mu_0$) object D , which is located in a rectangular waveguide with dimensions $a \times b$, having unknown inhomogeneous object function $v(r)$ where $r = (x, y, z)$ denotes position vector of any point in waveguide. The object function, namely, contrast of the object carries full information of electromagnetic properties of object D and could be complex if the material is lossy.

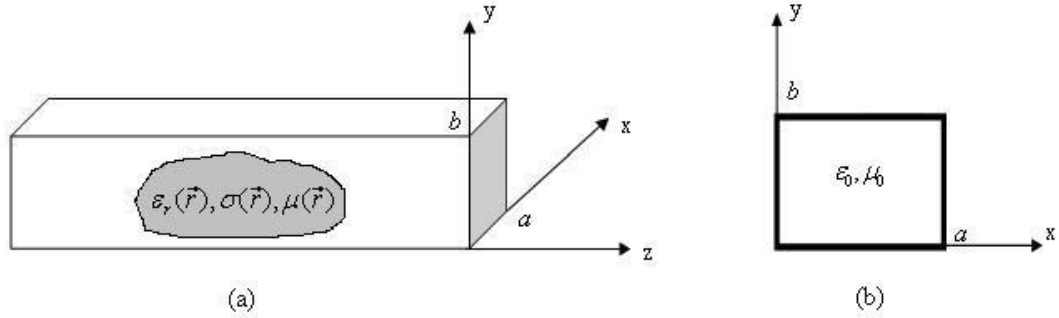


Figure 1.1 : Geometry of the problem: An inhomogeneous material which is placed in a rectangular waveguide (a) longitudinal view (b) cross-section view.

The unknown object function $v(r)$ can be defined in terms of constitutive parameters as

$$v(r) = \frac{k^2(r)}{k_0^2} - 1, \quad (2.1)$$

$$k^2(r) = \begin{cases} \omega^2 \epsilon_r(r) \epsilon_0 \mu_0 + i\omega \sigma(r) \mu_0, & r \in D; \\ \omega^2 \epsilon_0 \mu_0, & r \notin D, \end{cases} \quad (2.2)$$

for a given angular frequency ω . Here, $k(r), \epsilon_r(r), \sigma(r), \epsilon_0, \mu_0$ denote wave number of any point in loaded waveguide, relative dielectric permittivity, conductivity, dielectric permittivity of free space and permeability of free space, respectively. As it can be observed from the definition, the object function is able to be classified as a function with compact support and its support is assumed to be known. However further integral equations are still valid without this assumption, it does not only

reduce the computational cost of the proposed method, but it also will improve the capabilities and the validation limits of the method as far as possible. Because, this assumption allows one to introduce the knowledge of the shape into the problem. In other words, problem is reduced to the solution of the object function in a domain where the object function does not equal to zero. Furthermore, this assumption is very acceptable for a guided wave problem in microwave frequencies in a practical perspective.

Let us denote the incident, scattered and total electric field vectors inside the waveguide by \vec{E}^{inc} , \vec{E}^s and \vec{E} , respectively. Here the incident field \vec{E}^{inc} corresponds to electric field vector inside the empty waveguide for a chosen exciting case, while \vec{E} is the total electric field in the waveguide which is loaded by an arbitrary shaped inhomogeneous dielectric material. Thus the field defined by

$$\vec{E}^s = \vec{E} - \vec{E}^{inc} \quad (2.3)$$

can be considered as the contribution of the inhomogeneous 3-D body to the total field. From the above definitions together with wave equation in waveguide and using Green's Theorem one can have the following system of integral equations which are also known as the data equation,

$$\vec{E}^s(r) = k^2 \int_D \overline{\overline{G}}(r, r') v(r') \vec{E}(r') dv, \quad r \notin D \quad (2.4)$$

and the object equation,

$$\vec{E}(r) = \vec{E}^{inc}(r) + k^2 \int_D \overline{\overline{G}}(r, r') v(r') \vec{E}(r') dv, \quad r \in D \quad (2.5)$$

where $\overline{\overline{G}}(r, r')$ denotes the dyadic Green's function of the empty rectangular waveguide whose explicit expression will be given in the next chapter. It should be noted that the waveguide problem whose geometrical configuration is given in Fig. 1 is represented by the system of integral equations given by (2.4) and (2.5), and therefore they can be used for solving both direct and inverse problems. In the direct problem, the function $v(r)$, i.e., material properties are known and the electric field distribution is to be determined at any point inside the waveguide, while in the inverse scattering problem, scattered field is assumed to be measured at certain

points inside the waveguide but also outside the inhomogeneous object and is used to find the object function $v(r)$.

2.2 Dyadic Green's Function of Empty Rectangular Waveguide

Dyadic Green's function was firstly treated by Tai [18] with an error which was corrected again by same author [19]. Furthermore, in the literature, it is possible to find many techniques to construct the dyadic Green's function of empty rectangular waveguide and their closed or explicit expressions as well. Here, we just give an explicit expression of it in the following long form

$$\bar{\bar{G}}(r, r') = \bar{\bar{G}}_0(r, r') - \frac{1}{k_0^2} \bar{e}_z \bar{e}_z \delta(r - r') \quad (2.6)$$

In this equation, $r = (x, y, z)$ and $r' = (x', y', z')$ represents observation and source points respectively. \bar{e}_z is the unit vector for z direction and $\delta(r - r')$ is three-dimensional Dirac delta function. In (2.6), $\bar{\bar{G}}_0(r, r')$ is defined as

$$\bar{\bar{G}}_0(r, r') = \frac{i}{2abk_0^2} \sum_{m=0}^{\infty} \sum_{n=0}^{\infty} \frac{\lambda_m \lambda_n}{k_{mn}} e^{ik_{mn}|z-z'|} \left\{ \begin{array}{l} G_{0xx} \bar{e}_x \bar{e}_x + G_{0xy} \bar{e}_x \bar{e}_y + G_{0xz} \bar{e}_x \bar{e}_z + \\ G_{0yx} \bar{e}_y \bar{e}_x + G_{0yy} \bar{e}_y \bar{e}_y + G_{0yz} \bar{e}_y \bar{e}_z + \\ G_{0zx} \bar{e}_z \bar{e}_x + G_{0zy} \bar{e}_z \bar{e}_y + G_{0zz} \bar{e}_z \bar{e}_z \end{array} \right\} \quad (2.7)$$

where

$$G_{0xx} = [k_0^2 - (\frac{m\pi}{a})^2] \cos \frac{m\pi x}{a} \cos \frac{m\pi x'}{a} \sin \frac{n\pi y}{b} \sin \frac{n\pi y'}{b} \quad (2.8)$$

$$G_{0xy} = -(\frac{m\pi}{a})(\frac{n\pi}{b}) \cos \frac{m\pi x}{a} \sin \frac{m\pi x'}{a} \sin \frac{n\pi y}{b} \cos \frac{n\pi y'}{b} \quad (2.9)$$

$$G_{0xz} = \pm ik_{mn} (\frac{m\pi}{a}) \cos \frac{m\pi x}{a} \sin \frac{m\pi x'}{a} \sin \frac{n\pi y}{b} \sin \frac{n\pi y'}{b}, \quad z > z' \quad (2.10)$$

$$G_{0yx} = -(\frac{m\pi}{a})(\frac{n\pi}{b}) \sin \frac{m\pi x}{a} \cos \frac{m\pi x'}{a} \cos \frac{n\pi y}{b} \sin \frac{n\pi y'}{b} \quad (2.11)$$

$$G_{0yy} = [k_0^2 - (\frac{n\pi}{b})^2] \sin \frac{m\pi x}{a} \sin \frac{m\pi x'}{a} \cos \frac{n\pi y}{b} \cos \frac{n\pi y'}{b} \quad (2.12)$$

$$G_{0yz} = \pm ik_{mn} (\frac{n\pi}{b}) \sin \frac{m\pi x}{a} \sin \frac{m\pi x'}{a} \cos \frac{n\pi y}{b} \sin \frac{n\pi y'}{b}, \quad z > z' \quad (2.13)$$

$$G_{0zx} = \pm ik_{mn} (\frac{m\pi}{a}) \sin \frac{m\pi x}{a} \cos \frac{m\pi x'}{a} \sin \frac{n\pi y}{b} \sin \frac{n\pi y'}{b}, \quad z < z' \quad (2.14)$$

$$G_{0zy} = \pm i k_{mn} \left(\frac{n\pi}{b}\right) \sin \frac{m\pi x}{a} \sin \frac{m\pi x'}{a} \sin \frac{n\pi y}{b} \cos \frac{n\pi y'}{b}, \quad z < z' \quad (2.15)$$

$$G_{0zz} = \left[\left(\frac{m\pi}{a}\right)^2 + \left(\frac{n\pi}{b}\right)^2 \right] \sin \frac{m\pi x}{a} \sin \frac{m\pi x'}{a} \sin \frac{n\pi y}{b} \sin \frac{n\pi y'}{b} \quad (2.16)$$

$$\lambda_n = \begin{cases} 1, & n = 0 \\ 2, & n \neq 0 \end{cases} \quad (2.17)$$

$$k_{mn} = \sqrt{k_0^2 - k_c^2} \quad (2.18)$$

$$k_c^2 = \left(\frac{m\pi}{a}\right)^2 + \left(\frac{n\pi}{b}\right)^2 \quad (2.19)$$

2.3 Discretisation

In order to solve numerically one of the either direct or inverse problem which is defined by integral equations (2.4) and (2.5), Method of Moments is applied for discretisation of mentioned integral equations. To this aim, a kind of current source distribution -except a complex constant factor- as the multiplication of the total electric field vector and the object function is introduced such as

$$\Phi(r) = v(r)E(r) \quad (2.20)$$

Now, one can rewrite data and object integral equations in a compact form, respectively as follows

$$E^s = G^D \Phi \quad (2.21)$$

$$E = E^{inc} + G^O \Phi \quad (2.22)$$

Shortly, point matching technique which is one of the most used one in Method of Moments procedure is attempted for discretization of the data and object equations for numerical calculations. To this aim, domain D is divided into N equal rectangular prismatic cells. The current density is assumed to be uniform inside each cell, namely, $\Phi(r_n)$ where r_n represents the center of n th cell. So, one can represents the current density as follows

$$\Phi(r) = \sum_{k=1}^3 \sum_{n=1}^N \Phi_n^k B_n^k(r) \quad (2.23)$$

Here, $k=1,2,3$ denotes x, y, z and B_n^k is basis function defined as

$$B_n^k(r) = u_k P_n(r) \quad (2.24)$$

where u_k is unit vector and

$$P_n(r) = \begin{cases} 1, & \text{for } r \in \Delta D_n \\ 0, & \text{otherwise} \end{cases} \quad (2.25)$$

The weighting function is defined as

$$W_l^p(r) = \delta(r - r_l) u_p \quad (2.26)$$

The scalar product between f and g is defined as

$$\langle f, g \rangle = \int_V f \cdot g \, dv \quad (2.27)$$

Now, one can generate set of linear equations by first substituting into one of the integral equations, i.e., data equation and performing a scalar product on the resulting equation with the weighting function. This procedure leads the following set of equations

$$\sum_{k=1}^3 \sum_{n=1}^N \Phi_n^k A_{n,k}^{p,l} = C^{p,l} \quad (2.28)$$

where

$$C^{p,l} = E^s(r_{p,l}) \quad (2.29)$$

$$A_{n,k}^{p,l} = k^2 \int_{\Delta D_n} G(r_{p,l}, r'_{n,k}) \, dv \quad (2.30)$$

Very familiar procedure could be followed for the object equation additionally with a partial summation technique [20] that should be applied when calculating integration of Green's function for the case observation and source point are sama point, namely, $r=r'$. In this case, simple truncation of the series is inadequate for convergence of series appearing in the integration of dyadic Green's function. Therefore, these slowly convergent series are directly calculated by the aid of analytical formulas for infinite series. Explicit expression of the integration of dyadic Green's function even before applying partial summation technique is too complex and giving these formulas would go beyond the scope of the study. So, interested readers are referred to [20] for the details.

3. INVERSE SCATTERING

In this section, in order to reconstruct the object function of the material located in a rectangular waveguide, an iterative algorithm in the sense of Newton will be presented. In this sense, it is suitable to rewrite current density relation, the data and the object equation in operator form with full index.

$$\Phi_{j,\pm m}(r) = v_j(r)E_{j,\pm m}(r), \quad j=1,2,\dots,J \quad m=1,2,\dots,M \quad (3.1)$$

$$E_{j,\pm m}^s = G_j^D \Phi_{j,\pm m}, \quad j=1,2,\dots,J \quad m=1,2,\dots,M \quad (3.2)$$

$$E_{j,\pm m} = E_{j,\pm m}^{inc} + G_j^O \Phi_{j,\pm m}, \quad j=1,2,\dots,J \quad m=1,2,\dots,M \quad (3.3)$$

Here, m denotes the index of propagating modes, while positive sign represents modes which travel in $+z$ direction, negative sign represent modes which travel in $-z$ direction. Also index j is used to represent different frequencies within a chosen exciting frequency band. Since the imaginary part of the object function is depend on the frequency it will be convenient to use the following normalization

$$v_j(r) = \text{Re}[v_1] + i \frac{\omega_1}{\omega_j} \text{Im}[v_1], \quad j=1,2,\dots,J \quad (3.4)$$

In (3.4), the normalization procedure is realized with respect to the first frequency.

3.1 Initial Guess

Determination of an accurate initial guess for any Newton based iterative technique is a vital step. Because, Newton method uses Taylor expansion about a point which corresponds to initial value for the first iteration of Newton method and Taylor expansion gives healthy results around this point. Due the importance of initial values, instead of by trial and error, back-propagation algorithm that gives very satisfactory starting values is used. To this aim, normalized error in data equation, namely data error, is represented by a functional as follows:

$$F(\Phi_{j,\pm m,0}) = \frac{\sum_{j,\pm m} \|E_{j,\pm m}^s - G_j^D \Phi_{j,\pm m,0}\|^2}{\sum_{j,\pm m} \|E_{j,\pm m}^s\|^2} \quad (3.5)$$

Here, $\|\cdot\|$ denotes ℓ^2 norm. The gradient technique is used to minimize the functional, namely data error, one can write

$$\Phi_{j,\pm m,0} = \alpha_0 g_{j,\pm m,0} \quad (3.6)$$

$$g_{j,\pm m,0} = G_j^{D*} E_{j,\pm m}^s \quad (3.7)$$

where $g_{j,\pm m,0}$ denotes the gradient of the data operator, G_j^{D*} is the adjoint of data operator and α_0 is a constant that is to be determined by minimising the functional.

Then the initial guess for current density can be given by

$$\Phi_{j,\pm m,0} = \frac{\|G_j^{D*} E_{j,\pm m}^s\|^2}{\|G_j^D G_j^{D*} E_{j,\pm m}^s\|^2} G_j^{D*} E_{j,\pm m}^s \quad (3.8)$$

It should be noted that adjoint of data operator G_j^{D*} maps scattered field into domain of the object D , in other words it maps in opposite direction of data operator. That is why this technique is so called back-propagation. Then one can easily obtain initial guess of total electric field by using object equation such as

$$E_{j,\pm m,0} = E_{j,\pm m}^{inc} + G_j^O \Phi_{j,\pm m,0} \quad (3.9)$$

Final step of this chapter is to determine starting values for the object function via current density relation. It should be noted that while the total electric field and current density are vectorial functions, the object function is a scalar function. So the current density relation is an overdetermined system even if both single frequency and single mode propagation in only one direction are used to excite the waveguide. Also, forcing initial guess of the object function to be a complex constant is a suitable way to avoid unstable values which may lead divergent results in the application of the Newton method. In order to obtain a stable solution, least square regularization in the case the object function is forced to be a complex constant can be given by

$$\text{Re}[v_{1,0}] = \frac{\sum_{j,\pm m,n,k} \text{Re}[\Phi_{j,\pm m,n,k,0} \bar{E}_{j,\pm m,n,k,0}]}{\sum_{j,\pm m,n,k} E_{j,\pm m,n,k,0} \bar{E}_{j,\pm m,n,k,0}}, \quad \begin{array}{l} n=1,2,\dots,N \\ k=1,2,3 \end{array} \quad (3.10)$$

$$\text{Im}[v_{1,0}] = \frac{\sum_{j,\pm m,n,k} \left(\frac{\omega_1}{\omega_j}\right) \text{Im}[\Phi_{j,\pm m,n,k,0} \bar{E}_{j,\pm m,n,k,0}]}{\sum_{j,\pm m,n,k} \left(\frac{\omega_1}{\omega_j}\right)^2 E_{j,\pm m,n,k,0} \bar{E}_{j,\pm m,n,k,0}}, \quad \begin{array}{l} n=1,2,\dots,N \\ k=1,2,3 \end{array} \quad (3.11)$$

Here, overbar, $k=1,2,3$ and $n=1,2,\dots,N$ denote complex conjugate, unit vectors x, y, z and the number of subcells of the discretized volume of the object under test, respectively.

3.2 Newton Based Reconstruction Algorithm

Using the initial values obtained in previous section, one can formulate an iterative algorithm in the sense of Newton by using two term Taylor Expansion of nonlinear data operator with respect to the object function which leads the following linearized equation

$$G_j^D \Phi_{j,\pm m,0} + G_j^{D'} \Delta \Phi_{j,\pm m,0} = E_{j,\pm m}^s \quad (3.12)$$

where

$$\Delta \Phi_{j,\pm m,0} = E_{j,\pm m,0} \Delta v_j \quad (3.13)$$

and $G_j^{D'}$ is the Frechet derivative of data operator G_j^D with respect to the object function v_j and its explicit expression can be given by

$$G_j^{D'} \Delta \Phi_{j,\pm m,0} = k_j^2 \int_D \bar{G}_j(r, r') \bar{E}_{j,\pm m,0}(r') \Delta v_j(r') dv, \quad r \notin D. \quad (3.14)$$

Here the function Δv denotes the update amount of the object function. At this point, let us look through what well-posed means. According to Hadamard [21], a problem for which (i) there exist a solution (existence), (ii) there is at most one solution (uniqueness) and (iii) the solution depends continuously on data (stability) is called well-posed. If a problem does not satisfies even one of three requirements above, it is called as ill-posed for which obtaining a stable solution is notably difficult. Furthermore, certain mathematical physics problems such as inverse problems belong to this classification.

Roughly speaking, the equation (3.12) is an integral equation of first kind, from Fredholm Theory, this integral equation is severely ill-posed just as the other inverse problems. Herein, uniqueness may be very interesting question but this question is strictly out of scope of this study that merely aims to obtain a stable solution. So, Tikhonov regularization which simply replaces ill-posed first kind integral equation by a nearby well-posed integral equation of the second kind [22] is applied to obtain a stable solution as follows

$$\Delta\Phi_{j,\pm m,0}^\alpha = [\alpha I + G_j^{D'*} G_j^{D'}]^{-1} [G_j^{D'*} (E_{j,\pm m}^s - G_j^D \Phi_{j,\pm m,0})] \quad (3.15)$$

where I is an identity operator and α is regularization parameter that is chosen according to discrepancy principle of Morozov which guarantees error due to regularization be equal or less than expected noise level δ [6], namely,

$$\|G_j^{D'} \Delta\Phi_{j,\pm m,0}^\alpha - (E_{j,\pm m}^s - G_j^D \Phi_{j,\pm m,0})\| \leq \delta \quad (3.16)$$

By using singular value decomposition of Frechet derivative of data operator $G_j^{D'} = USV^*$, also choosing $\alpha > 0$, one can obtain a monotonically increasing function,

$$f(\alpha) = \sum_i \frac{\alpha^2 - \delta^2 s_i^2}{(s_i^2 + \alpha^2)^2} |U^* (E_{j,\pm m}^s - G_j^D \Phi_{j,\pm m,0})|^2, \quad (3.17)$$

where $\{s_i\}$ singular values of Frechet derivative of data operator $G_j^{D'}$. Now, one can easily obtain regularization parameter by finding root of the monotonical function given in (3.17).

Once $\Delta\Phi_{j,\pm m,0}^\alpha$ as a function of update amount of the object function Δv is obtained via Newton method, one can solve the equation (3.13) in least square sense as follows,

$$\text{Re}[\Delta v] = \frac{\sum_{j,\pm m,k} \text{Re}[\Delta\Phi_{j,\pm m,k,0}^\alpha \bar{E}_{j,\pm m,k,0}]}{\sum_{j,\pm m,k} E_{j,\pm m,k,0} \bar{E}_{j,\pm m,k,0}}, \quad (3.18)$$

$$\text{Im}[\Delta v] = \frac{\sum_{j,\pm m,k} \left(\frac{\omega_1}{\omega_j}\right) \text{Im}[\Phi_{j,\pm m,k,0}^\alpha \bar{E}_{j,\pm m,k,0}]}{\sum_{j,\pm m,k} \left(\frac{\omega_1}{\omega_j}\right)^2 E_{j,\pm m,k,0} \bar{E}_{j,\pm m,k,0}}. \quad (3.19)$$

It should be noted that least square algorithm allows one to use all vector

components of fields, the data related to different frequencies and the additional data coming from the higher modes, simultaneously. As expected, this algorithm can be used to improve the capabilities of the method by increasing the number of operating frequencies and the modes. After obtaining Δv , the object function can be easily updated as

$$v_1 = v_0 + \Delta v. \quad (3.20)$$

Then the total electric field is updated through the object equation

$$E_{j,\pm m,1} = E_{j,\pm m}^{inc} + G_j^O(E_{j,\pm m,1} v_1). \quad (3.21)$$

In Newton method, the iteration is terminated when the norm of $\Delta v/v$ becomes smaller than a predefined real number or a predefined iteration number is reached. In this study, the two stopping rule are used together and the one which is satisfied early is used as the termination rule.

To summarize, iteration steps can be listed as follows

- I. Firstly, determine initial values for the object function $v_{1,0}$ and the total electric field $E_{j,\pm m,0}$ with the aid of backpropagation algorithm.
- II. In next step, solve the data equation to find $\Delta \Phi_{j,\pm m,0}^\alpha$ in Newton sense where Tikhonov regularization is applied to obtain a stable solution where regularization parameter is calculated by Morozov discrepancy rule.
- III. Solve the overdetermined equation $\Delta \Phi_{j,\pm m,0}^\alpha = \Delta v E_{j,\pm m,0}$ in a least square sense and update object function.
- IV. Then update the total electric field via object equation.
- V. Iterations (steps from II to IV) continue until one of stopping rule is satisfied

3.3 Numerical and Experimental Results

In this section, some numerical and experimental results are presented in order to validate the method as well as to see the effects of some parameters on the results. In all simulations, cross section of the waveguide is chosen as $a=7.2cm$ and $b=3.2cm$.

To be able to model more realistic cases, a random term

$$\tilde{E}_{j,\pm m,k}^s = E_{j,\pm m,k}^s + \xi |E_{j,\pm m,k}^s| e^{i2\pi r_n} \quad (3.22)$$

is added to simulated data, where ξ is the noise level that is also used as expected

noise level for Morozov's rule and r_n 's are normally distributed random numbers in the interval $[0,1)$. Iterations are terminated when one of the stopping rules is satisfied such that $\|\Delta v\|/\|v_n\| < 10^{-3}$ and iteration number reached at 256.

As a first example, the proposed method is applied to an inhomogeneous lossy dielectric rectangular prism which is placed in $(x, y, z) \in [2, 4] \times [0, 2] \times [0, 4] \text{cm}^3$. The real and imaginary parts of the object function of the material under test vary linearly and sinusoidally along the z -axis, respectively. The number of cells and noise level are chosen as $N=5 \times 5 \times 10=250$ cells and $\xi=0.01$. The reflected and transmitted field are assumed to be measured at two points defined by $(x, y, z)=(a/2, b/2, \pm 15 \text{cm})$. Exact and reconstructed variations of real and imaginary parts of the object function are given in Fig 3.1 and Fig 3.2 for the operating frequency $f=2.5 \text{GHz}$ which allows only dominant mode TE_{10} to propagate. Clearly, the results show that the method gives satisfactory reconstruction for smoothly varying profiles even with only four data. In the second example, a three layered dielectric material which is placed in $(x, y, z) \in [2, 3.2] \times [0, 1.2] \times [0, 4.5] \text{cm}^3$ is considered. The reflected and transmitted field are again assumed to be measured at two points defined by $(x, y, z)=(a/2, b/2, \pm 15 \text{cm})$. The number of operating frequency is $J=9$ in a range of $f=2.5-3.5 \text{GHz}$. The obstacle is divided into $N=5 \times 5 \times 12=300$ cells and noise level $\xi=0.03$. Through the results that are presented in Fig 3.3 and Fig 3.4, it can be observed that the method is not capable of sharp transition, but gives a smoothed approximation of the actual profile.

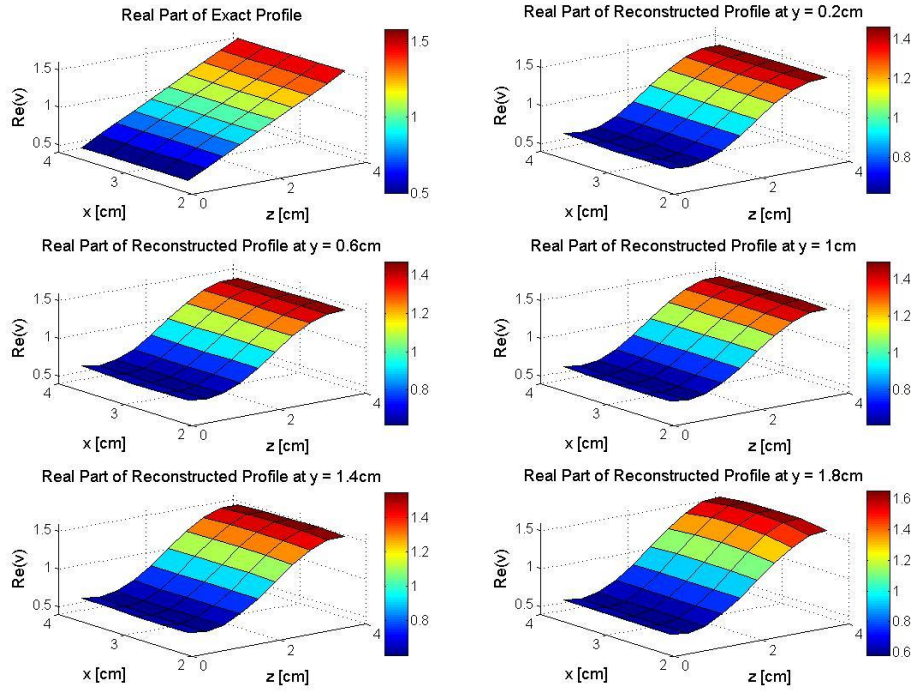


Figure 3.1 : Exact and reconstructed profiles of an inhomogeneous material having linearly varying real part for five different y slices.

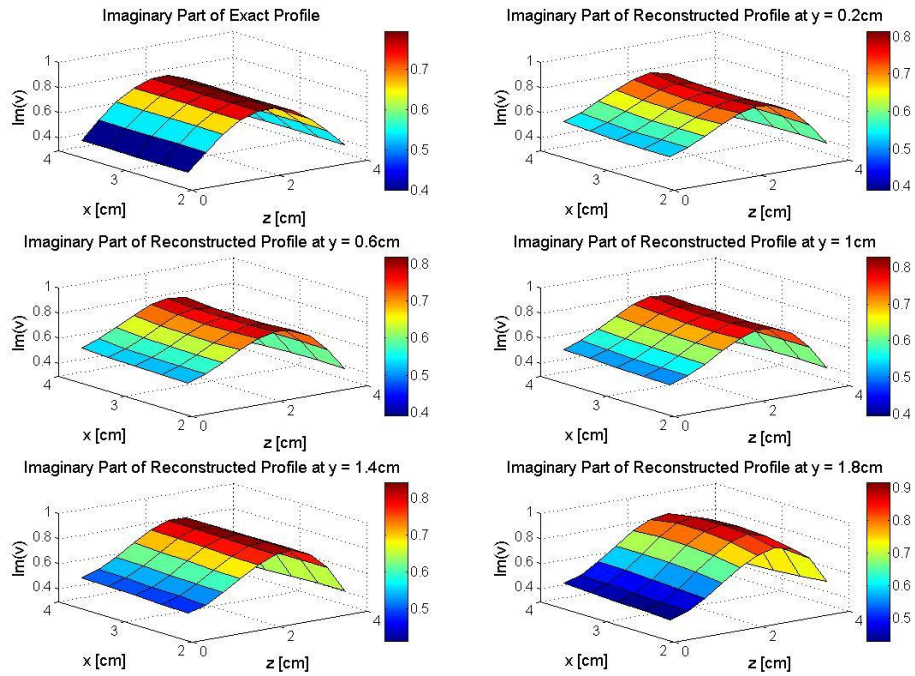


Figure 3.2 : Exact and reconstructed profiles of an inhomogeneous material having linearly varying imaginary part for five different y slices.

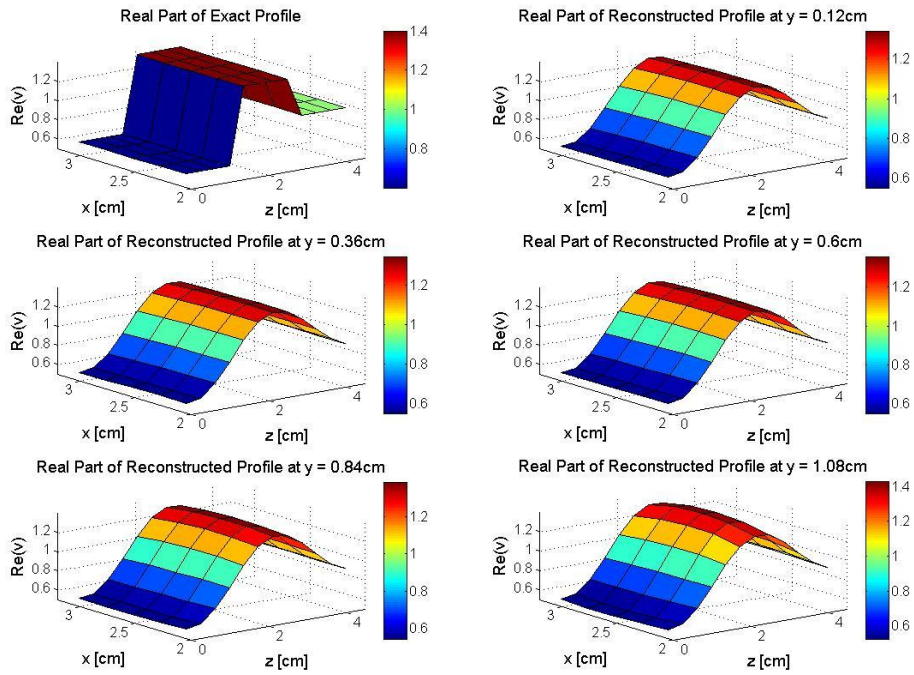


Figure 3.3 : Exact and reconstructed profiles of three layer material : real part for five different y slices.

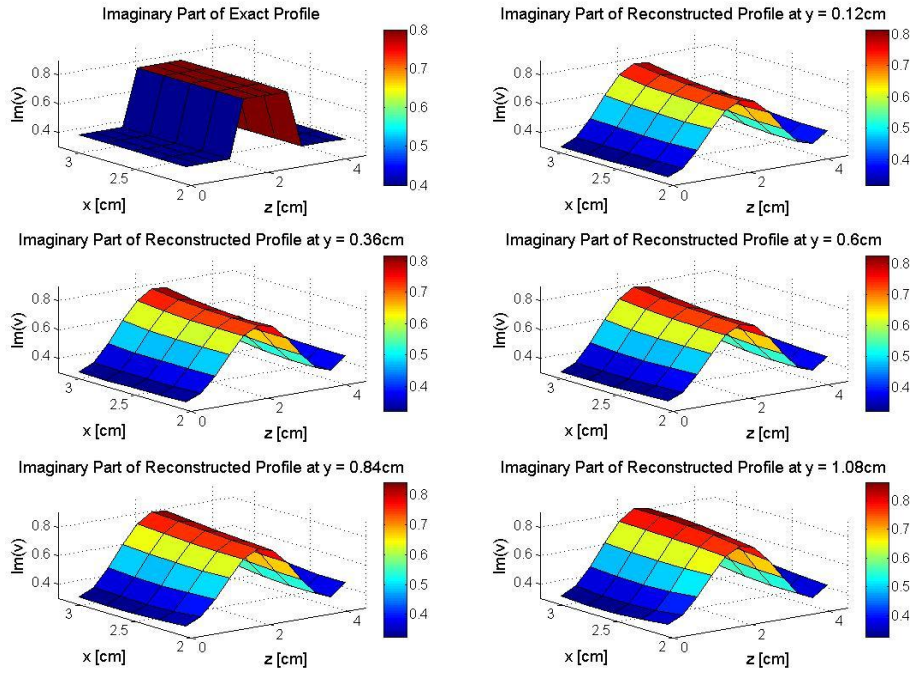


Figure 3.4 : Exact and reconstructed profiles of three layer material : imaginary part for five different y slices.

In the third example, a lossless dielectric material which has 2-D sharp variation and is placed in $(x, y, z) \in [1, 2.2] \times [0, 0.6] \times [1, 2.2] \text{cm}^3$ is considered. Operating frequency is 6GHz which allows the multi-mode propagation. So, it is not meaningful to measure the scattered field at one point and it is assumed that the reflected and transmitted field are measured at equidistant $4 \times 3 = 12$ points defined in the regions $(x, y) \in [1.5, 4.5] \times [1, 3] \text{cm}^2, z = \pm 15\text{cm}$. The exact and reconstructed profiles are given in Fig 3.5 for which the obstacle divided into $N = 10 \times 5 \times 10 = 500$ cells and noise level $\xi = 0.03$. From numerical examples, multi frequency measurement does not improve the results for the given parameters, while the results start to deteriorate for higher noise level. In order to see the effects of multi-frequency measurement in the case of higher noise level, the previous example is repeated with same parameters except for the noise level $\xi = 0.1$, The number of operating frequency is $J = 6$ in a range of $f = 6 - 7\text{GHz}$ and the results are given in Fig 3.6. Through the last two example, one can conclude that the method gives only a rough approximation of actual profiles and however, multi-frequency measurement is not an efficient tool to improve the resolution of the results, one can use multi-frequency measurement in the case of high noise level to obtain stable solution. The final configuration of third example is devoted to show that the reconstruction quality can be enhanced by using higher frequencies, especially for sharp variations. Thus, we reconsider the profile in the previous example and apply the method for a single frequency of $f = 10\text{GHz}$. The scattered data is assumed to be measured equidistant $6 \times 5 = 30$ in the regions $(x, y) \in [1, 6] \times [1, 3] \text{cm}^2, z = \pm 15\text{cm}$ and contaminated with a noise level $\xi = 0.03$ and the obstacle divided into $N = 12 \times 5 \times 12 = 720$ cells. The results given in Fig 3.7 showed that in higher frequency case, the method gives more satisfactory reconstruction rather than in lower frequency case.

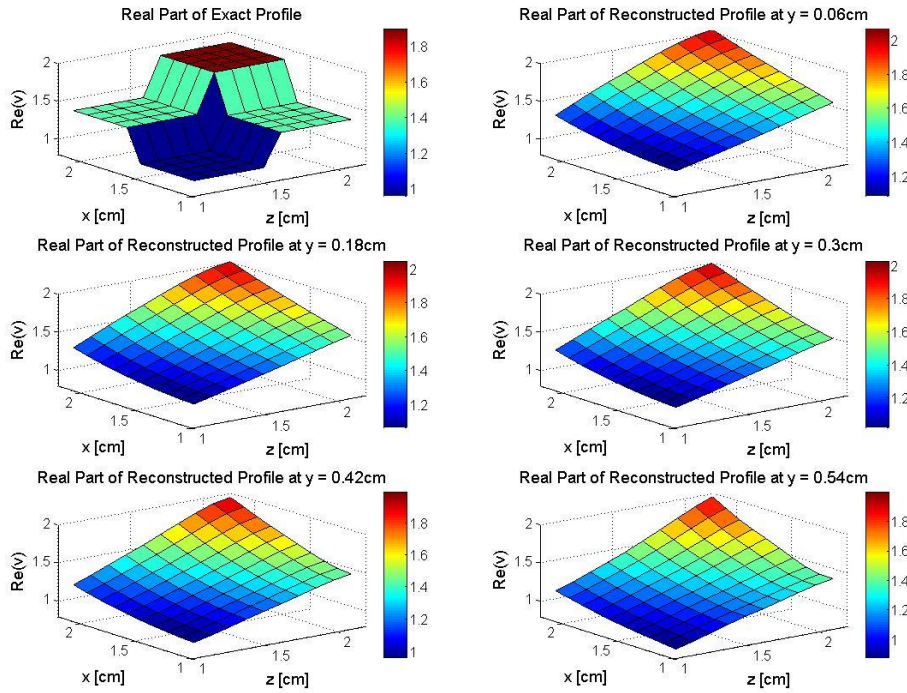


Figure 3.5 : Exact and reconstructed profiles of an inhomogeneous material having 2-D sharp variations for $\xi=0.03$ and $6GHz$.

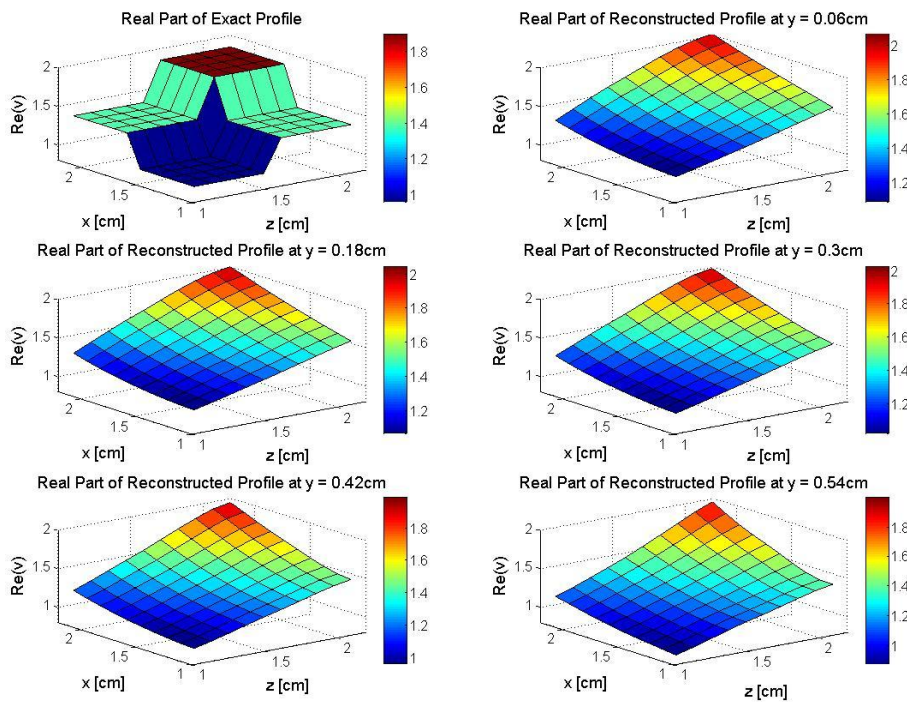


Figure 3.6 : Exact and reconstructed profiles of an inhomogeneous material having 2-D sharp variations for $\xi=0.1$ and $J=6$ in range of $f=6-7GHz$.

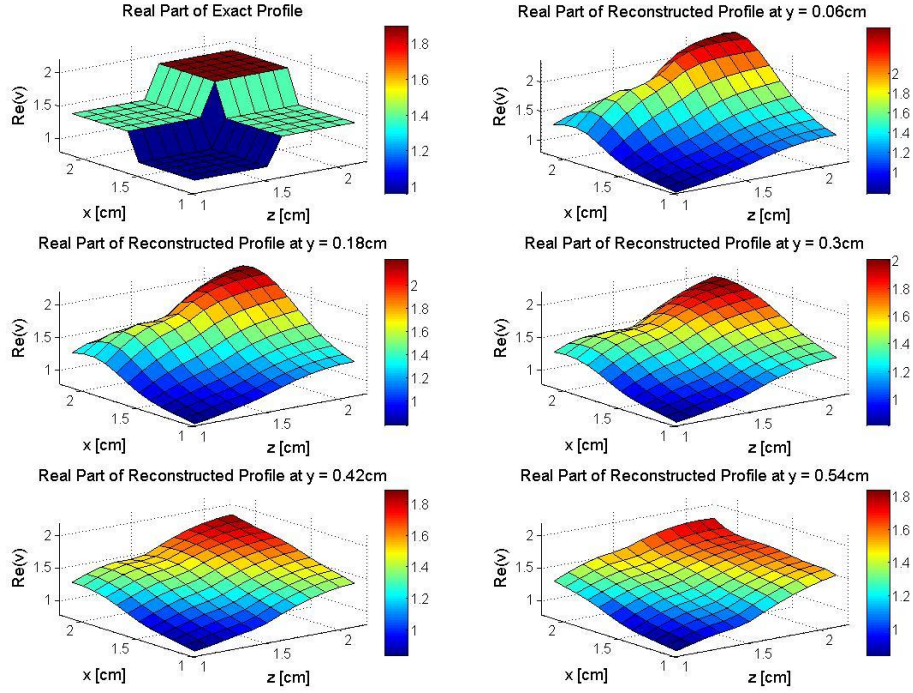


Figure 3.7 : Exact and reconstructed profiles of an inhomogeneous material having 2-D sharp variations for $\xi=0.03$ and $9GHz$.

Lastly, the proposed method is tested against experimental data. To this aim, a homogeneous material (teflon) is located in $(x, y, z) \in [0, 7.2] \times [0, 1.7] \times [-0.5, 0.5] cm^3$ in a rectangular waveguide, cross section of which is $a=7.2cm$ and $b=3.4cm$. S_{11} and S_{21} parameters are measured at $z = \pm 15.24cm$ for $J=11$ frequencies between $f=2.7-3.7GHz$. Since S_{12} and S_{22} are not measured, fields propagating in $+z$ direction are only taken into account. After applying a suitable calibration, it is easy to convert S-parameters into scattered fields. The obstacle is divided into $N=12 \times 5 \times 12 = 720$ cells and expected noise level is chosen as $\delta=0.02$. In Fig 3.8 and Fig 3.9, real and imaginary part of reconstructed permittivities ($\epsilon_r = v+1$) are demonstrated. By considering that real part of the object function of teflon is between 1.0 – 1.1 and imaginary part is about 0.001, the results are quite satisfactory. It should be noted that backpropagation algorithm gives very good initial guess and in order to see the results in the case of poorly initial guess, the reconstruction is repeated without using back-propagation algorithm and initial guess is chosen as $v_0=0.5+i0$. For this case, the results are plotted in Fig 3.10 and 3.11 and it is observed that the method gives still satisfactory reconstruction.

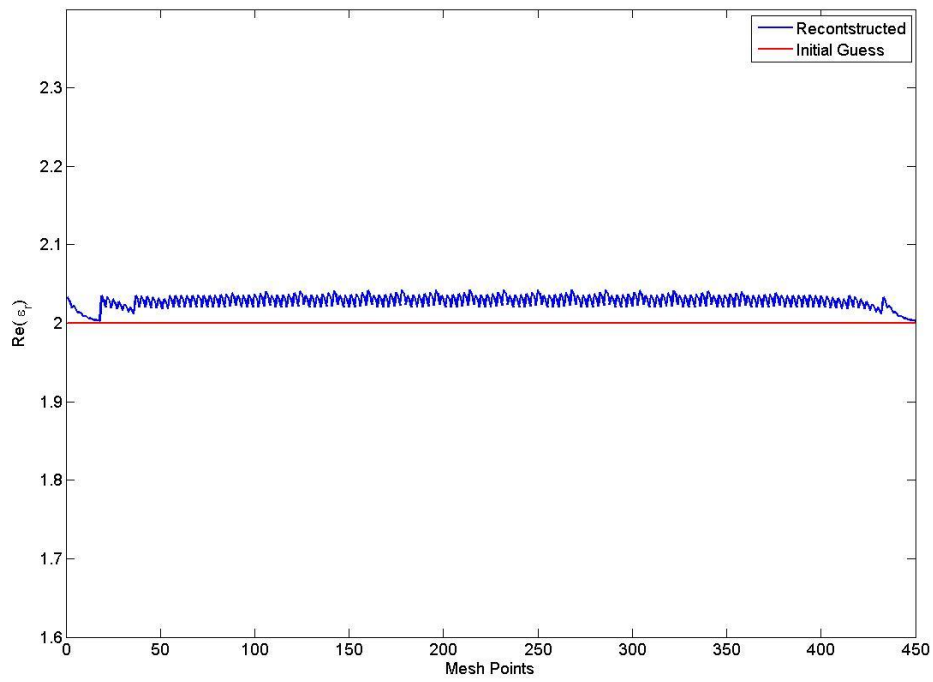


Figure 3.8 : Real part of reconstructed versus mesh points when backpropagation algorithm is used.

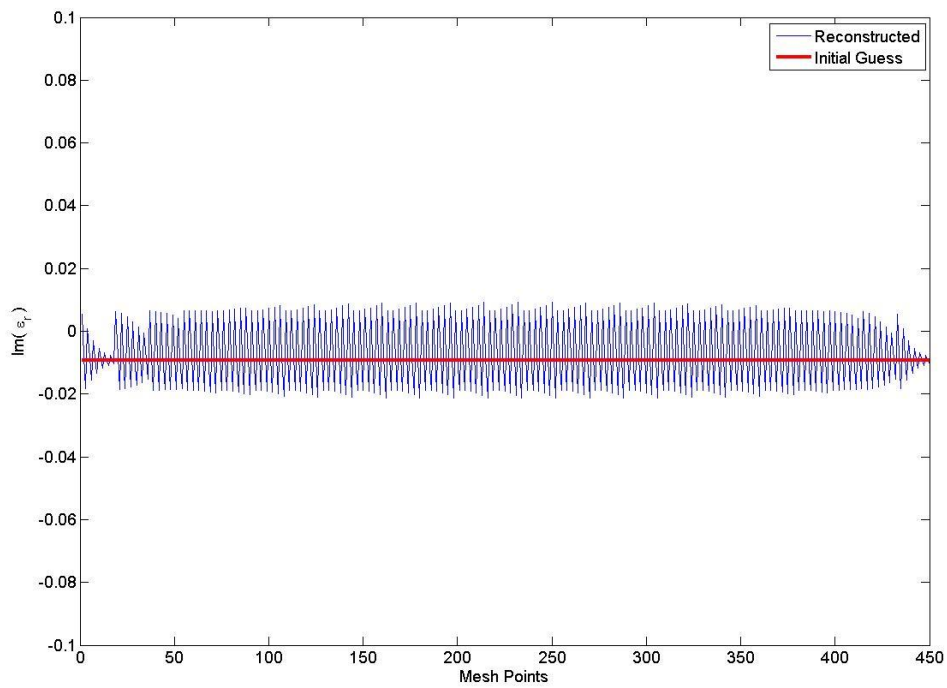


Figure 3.9 : Imaginary part of reconstructed mesh points versus mesh points when backpropagation algorithm is used.

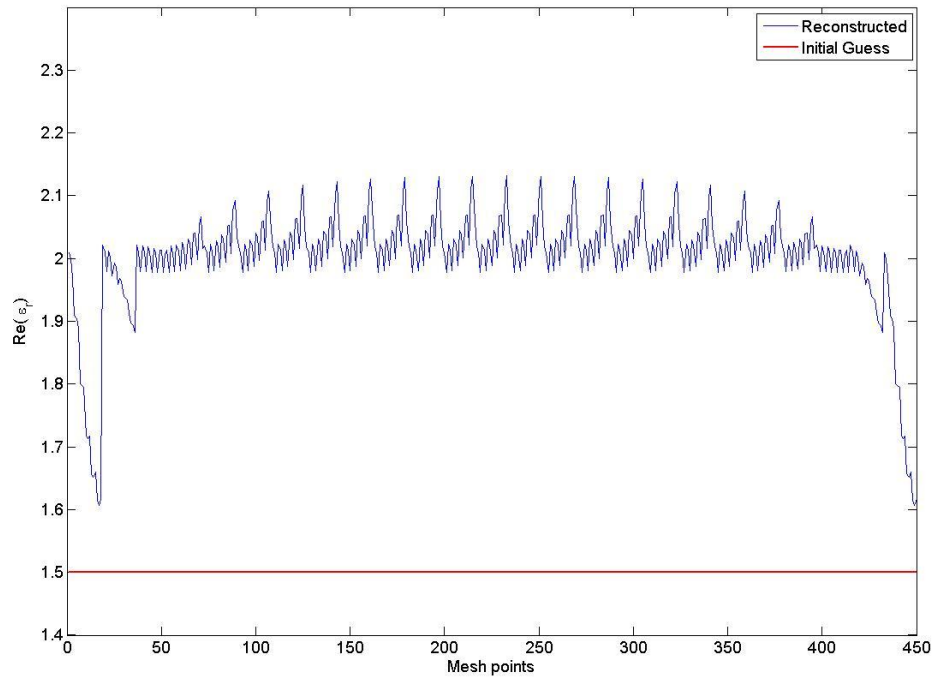


Figure 3.10 : Real part of reconstructed versus mesh points when initial guess is chosen manually.

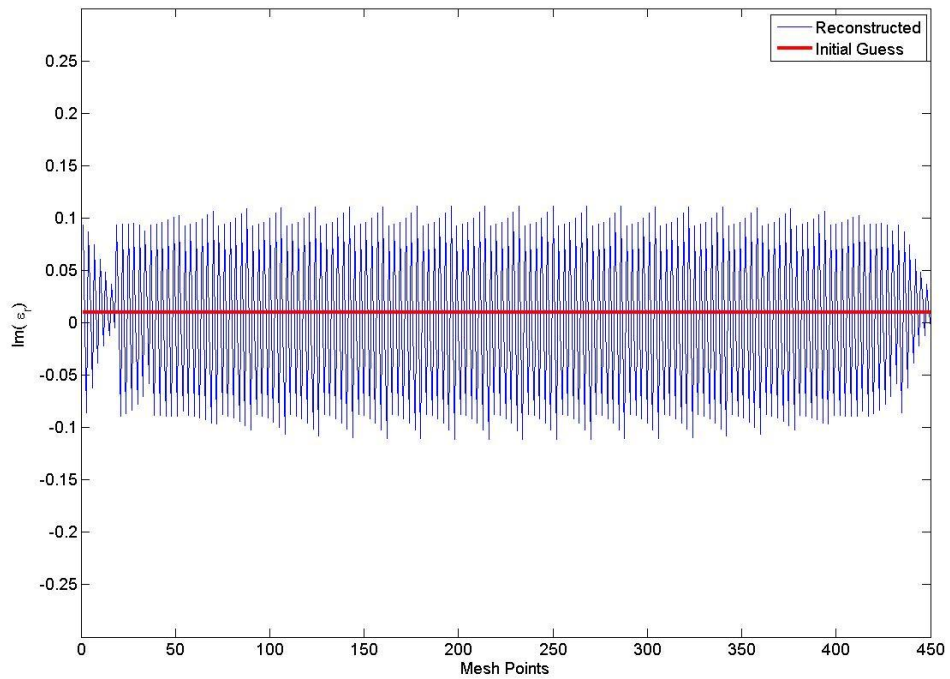


Figure 3.11 : Imaginary part of reconstructed versus mesh points when initial guess is chosen manually.

4. CONCLUSION

In this thesis, 3-D nonlinear inverse scattering of guided waves is investigated by an iterative method based on Newton algorithm. The problem is formulated via two well-known integral equations by the aid of dyadic Green's function of empty rectangular waveguide. Then the problem is reduced to a nonlinear equation in terms of the unknown object function which is solved iteratively via Newton method together with a regularization in the sense of Tikhonov and Morozov's rule for determining regularization parameter. For numerical implementations, infinite dimensional operators are projected onto a finite dimensional ones by following a simple Method of Moments technique, namely, point matching procedure. Numerical examples show that the proposed method gives very satisfactory reconstruction for smoothly varying profiles, although the method gives only a rough approximation of the actual profile for sharp profiles. It is also observed that the method is very sensitive to the noisy data in single frequency measurement case. However this sensitivity can be readily reduced by the use of multi-frequency measurements, as shown in numerical results. Another issue that is worth noting is that the resolution of the method can be enhanced by using higher frequencies for the profiles having abrupt changes in their geometrical or physical properties. Furthermore, the method is tested against real data for homogeneous case. However, primary experimental results are hopeful, experiments are not good enough to demonstrate the capabilities of the method. So, many experiments should be performed for various cases and further studies will be developed in this direction.

REFERENCES

- [1] **Tijhuis, A. G.**, 1989: Born-type reconstruction of material parameters of an inhomogeneous lossy dielectric slab from reflected-field data, *Wave Motion*, **11**, 151-173.
- [2] **Chew, W. C., and Wang, Y. M.**, 1990: Reconstruction of two dimensional permittivity distribution using the distorted Born iterative method, *IEEE Trans. Med. Imaging*, **9**, 218-225.
- [3] **Habashy, T. M., Gross, R. W., and Spies, B. R.**, 1993: Beyond the Born and Rytov approximations, a nonlinear approach to electromagnetic scattering, *J. Geophys. Res.*, **98**, 1759–1775.
- [4] **Roger, A.**, 1981: A Newton-Kantorovich algorithm applied to an electromagnetic inverse problem, *IEEE Trans Ant. Prop.*, **29**, 232-238.
- [5] **van den Berg, P. M., and Kleinman, R. E.**, 1997: A Contrast source inversion method, *Inverse Problems*, **13**, 1607-1620.
- [6] **Colton, D., Coyle, J., and Monk, P.**, 2000: Recent Developments in Inverse Acoustic Scattering Theory, *SIAM Review*, **42**, 369-414.
- [7] **Caorsi, S., Massa, A., and Pastorino M.**, 2000: A computational technique based on a real-coded genetic algorithm for microwave imaging purposes, *IEEE Trans. Geo. Remote Sensing*, **38**, 1697-1708.
- [8] **Caorsi, S., and Gamba, P.**, 1999: Electromagnetic detection of dielectric cylinders by a neural network approach, *IEEE Trans. Geo. Remote Sensing*, **37**, 820-827.
- [9] **Dediu, S., and McLaughlin, J. R.**, 2006: Recovering inhomogeneities in a waveguide using eigensystem decomposition, *Inverse Problems*, **22**, 1227-1246.
- [10] **Bourgeois, L., and Luneville, E.**, 2007: The linear sampling method in a waveguide: a modal formulation, *Inverse Problems*, **24**, 015018.
- [11] **Simsek, S., Isik, C., Topuz, E., and Esen, B.**, 2006: Electromagnetic detection of dielectric cylinders by a neural network approach, *AEU-Int. J. Elec. Comm.*, **60**, 677-680.
- [12] **Baginski, M. E., Faircloth, D. L., and Deshpande, M. D.**, 2005: Comparison of two optimization techniques for the estimation of complex permittivities of multilayered structures using waveguide measurements, *IEEE Trans. Microw. Theory Tech*, **53**, 3251-3259.
- [13] **Faircloth, D. L., Baginski, M. E., and Wentworth, S. M.**, 2006: Complex permittivity and permeability extraction for multilayered samples using S-parameter waveguide measurements, *IEEE Trans. Microw. Theory Tech*, **54**, 1201-1209.

- [14] **Akleman, F.**, 2008: Reconstruction of complex permittivity of a longitudinally inhomogeneous material loaded in a rectangular waveguide *IEEE Microw. Wireless Compon. Lett.*, **18**, 158-160.
- [15] **Requena-Prez M. E., Albero-Ortiz, A., Monz-Cabrera, J., and Daz-Morcillo, A.**, 2006: Combined use of genetic algorithms and gradient descent optimization methods for accurate inverse permittivity, *IEEE Trans. Microw. Theory Tech*, **54**, 615-624.
- [16] **Brovko, A. V., Murphy, E. K., and Yakovlev, V. V.**, 2009: Waveguide microwave imaging: Neural network reconstruction of functional 2-D permittivity profiles, *IEEE Trans. Microw. Theory Tech*, **57**, 406-414.
- [17] **van den Berg, P. M.**, 2002: Nonlinear Scalar Inverse Scattering: algorithms and applications, in *Scattering and Inverse Scattering in Pure and Applied Science*, **1**, p. 142-161, Eds. Pike, R., and Sabatier, P., Academic Press, London.
- [18] **Tai, C. T.**, 1971: *Dyadic Green's Functions in Electroamgnetic Theory*, Intext Educational Publishers, New York.
- [19] **Tai, C. T.**, 1972: On the Eigenfunction Expansion of Dyadic Green's Functions, *Proc. IEEE*, **61**, 480-481.
- [20] **Wang. J. H.**, 1978: Analysis of a three dimensional arbitrarily shaped dielectric or biological body inside a rectangular waveguide, *IEEE Trans. Microw. Theory Tech*, **26**, 457-462.
- [21] **Hadamard, J.**, 1923: *Lectures on Cauchy's problem in linear partial differential equations*, Yale University Press, New Haven, CT.
- [22] **Groetsch C. W.**, 2007: Integral equations of the first kind, inverse problems and regularization: a crash course, *J. Phys.: Conf. Ser*, **73**, 012001.

CURRICULUM VITA

Candidate's full name: Emre Kılıç

Place and date of birth: İstanbul, 26/02/1986

Permanent Address: Esatpaşa Mah. Mehmet Katip Sokak No: 22
Ataşehir/İSTANBUL

Universities and

Colleges attended: Istanbul Technical University,
Electrical and Electronics Faculty,
Telecommunications Engineering, 2008

Publications:

- **Kılıç E.**, Akleman F., Esen B., Özaltın D. M., Özdemir Ö., and Yapar A., 2010: 3-D imaging of inhomogenous materials loaded in rectangular waveguide. *IEEE Trans. Microw. Theory Tech*, **58**, 1290-1296.
- **Kılıç E.**, Çayören M., Yapar A., and Akduman I., 2009: Reconstruction of perfectly conducting rough surfaces by the use of inhomogeneous surface impedance modelling. *Inverse Problems and Imaging*, **3**, 295-307.
- **Kılıç E.**, Özaltın D. M., Akleman F., Yapar A., and Özdemir Ö., 2009: A Newton method for the reconstruction of complex permittivity of an inhomogenous material located in a rectangular waveguide. *The 9th International Conference on Mathematical and Numerical Aspects of Waves Propagation*, June 15-19, 2009 Pau, France
- Unal G.S., Semerci O., **Kılıç E.**, and Akduman I., 2009: Surface impedance reconstruction of an object located over a constant impedance surface. *Days on Diffraction 2009*, June 3-6, 2008 Petersburg, Russia.
- Unal G.S., Çayören M., and **Kılıç E.**, 2008: Determination of earth roughness through surface impedance modelling. *10th Specialist Meeting on Microwave Radiometry and Remote Sensing for the Enviroment*, March 11-14, 2008 Florence, Italy.